

Fullerenes, Nanotubes and Carbon Nanostructures

Publication details, including instructions for authors and subscription information:

<http://www.tandfonline.com/loi/lfn20>

SAXS Measurement and Dynamics of Condensed Carbon Growth at Detonation of Condensed High Explosives

K. A. Ten^a, E. R. Prueel^a & V. M. Titov^a

^a Lavrentyev Institute of Hydrodynamics, Siberian Branch of RAS, Novosibirsk, Russia

Available online: 14 May 2012

To cite this article: K. A. Ten, E. R. Prueel & V. M. Titov (2012): SAXS Measurement and Dynamics of Condensed Carbon Growth at Detonation of Condensed High Explosives, Fullerenes, Nanotubes and Carbon Nanostructures, 20:4-7, 587-593

To link to this article: <http://dx.doi.org/10.1080/1536383X.2012.656542>

PLEASE SCROLL DOWN FOR ARTICLE

Full terms and conditions of use: <http://www.tandfonline.com/page/terms-and-conditions>

This article may be used for research, teaching, and private study purposes. Any substantial or systematic reproduction, redistribution, reselling, loan, sub-licensing, systematic supply, or distribution in any form to anyone is expressly forbidden.

The publisher does not give any warranty express or implied or make any representation that the contents will be complete or accurate or up to date. The accuracy of any instructions, formulae, and drug doses should be independently verified with primary sources. The publisher shall not be liable for any loss, actions, claims, proceedings, demand, or costs or damages whatsoever or howsoever caused arising directly or indirectly in connection with or arising out of the use of this material.

SAXS Measurement and Dynamics of Condensed Carbon Growth at Detonation of Condensed High Explosives

K. A. TEN, E. R. PRUEEL AND V. M. TITOV

Lavrentyev Institute of Hydrodynamics, Siberian Branch of RAS, Novosibirsk,
Russia

Description of the method and results of the investigation of carbon condensation dynamics in the products of detonation of condensed explosives with high carbon content are presented. The method is based on the determination of the dynamics of small-angle X-ray scattering directly during the experimental explosion. For a series of explosive charges, for example, those based on TATB, the mixture of TNT50%+RDX50%, BTF, the time of the formation of condensed phase was estimated, and the dynamics of the average size of the nanoparticles of detonation carbon was determined.

Keywords Detonation nanodiamond, SAXS

Introduction

During the detonation of explosives with high carbon content, substantial fraction of the condensed residue is observed along with gaseous products of the explosion. The condensed residue is composed of carbon in different phase forms (Figure 1). Permanent attention to this problem is dictated, on the one hand, by the necessity to consider this feature for the description of detonation and explosive flows and, on the other hand, for technologically simple detonation synthesis of carbon nanoparticles including diamond ones. It is necessary to understand this phenomenon and, if possible, to govern the parameters of the resulting nanomaterials.

Along with this, the experimental determination of even the general kinetics of carbon condensation, without deciphering the geometric and phase structure of the particles formed under detonation, is connected with understandable difficulties. The published results of the comparison between calculated and experimental data on the acceleration of very thin metal plates by the products of detonation of explosives with negative oxygen balance showed that this process is described more accurately assuming carbon condensation beyond the zone of chemical reaction (1,2).

At present, one of the unique experimental methods of the dynamic registration of the formation of condensed carbon nanoparticles directly during the detonation of explosives is the diffraction method involving the synchrotron radiation (SR) (3). For this purpose, the method of measuring small-angle X-ray scattering (SAXS) was developed for dynamic systems. The method is based on the measurement of the scattered X-ray radiation directly during the explosion experiment.

Address correspondence to E. R. Prueel, Lavrentyev Institute of Hydrodynamics, Siberian Branch of RAS, Lavrentyevan – 15, 630090, Novosibirsk, Russia. E-mail: pru@hydro.nsc.ru

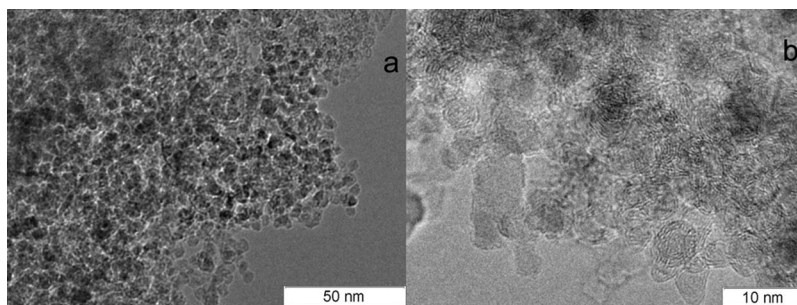


Figure 1. Condensed residue of carbon nanostructures collected after the explosion of trinitrotoluol (TNT)50%+hexogen(RDX)50% charge.

X-ray scattering is sensitive to the nonuniformities of the electron density, which is termed as the presence of the particles of condensed carbon in the gaseous products of explosion. Its intensity and angular distribution may be used to estimate the amount of condensed carbon and some average particle size.

A combination of SAXS involving SR from powerfully charged particle accelerators (VEPP-3, energy: 2 GeV, Institute of Nuclear Physics, SB RAS, Novosibirsk) allows one to perform dynamic measurements of the distribution of SAXS with the exposure of 1 ns and the periodicity of 250 ns.

SAXS Theory

SAXS allows one to determine the shapes and structures of nanoparticles. The particles may be solid, liquid or gaseous, but it is essential that their electron density differs from the density of the medium; that is, the method is sensitive to the “fluctuation of the electron density.”

According to the basic principles (4), to calculate small-angle scattering it is necessary to take interference from all electrons of the scattering object

$$\vec{E}(\vec{q}) \propto \int_V n(\vec{r}) e^{-i\vec{q}\cdot\vec{r}} d\vec{r} \quad (1)$$

where $\vec{q} = \vec{k} - \vec{k}_0 = 2k \sin(\theta/2) = \frac{4\pi \sin(\theta/2)}{\lambda}$ is the vector of scattering, \vec{k}_0 and \vec{k} are wave vectors of the incident and scattered radiation, λ is wavelength and θ is the angle of scattering.

If the scattering object is in a vacuum, then the electron density $n(\vec{r})$ is taken to be the usual density of the material of the object ($n \rightarrow \rho$). SAXS is sensitive to the density of the scattering substance.

If the scattering structure is not in vacuum but in a medium with the electron density n_0 , the amplitude of the wave will be proportional to $(n - n_0)$. In this situation, ($n \rightarrow \Delta\rho = (\rho - \rho_0)$).

Calculating the intensity of scattered radiation, the latter will be proportional to the difference in the densities of the medium and the object under investigation ($\Delta\rho^2$). SAXS is sensitive to density nonuniformities. The square of density difference $\Delta\rho^2$ is often termed “contrast.” In this work, the account of the latter is principally important for correct

determination of the amount of condensed carbon in explosion products, the density of which changes substantially during the experiment.

Without any additional assumptions concerning the structure of the isotropically scattering object, using $I(q)$ measured in the SAXS experiment, one can recover only the autocorrelation function of density nonuniformity $\gamma(\vec{r}) = \frac{1}{V} \int \Delta\rho(\vec{r}') \Delta\rho(\vec{r}' - \vec{r}) d\vec{r}'$. The

following relations are used here:

$$\gamma(r) = \frac{1}{2\pi^2} \int_0^\infty I(q) \frac{\sin(qr)}{qr} q^2 dq,$$

$$I(q) = 4\pi \int_0^\infty \gamma(r) \frac{\sin(qr)}{qr} r^2 dr \quad (2)$$

Analyzing the whole $\gamma(r)$, we will consider here only two moments. The first one links total intensity of the radiation scattered over the whole angle range with the total amount of the condensed scattering phase without distinguishing the sizes and shapes of the particles under investigation. From equation (2), for $r = 0$ we obtain

$$\gamma(0) = \int_V \Delta\rho^2(\vec{r}) dV \propto \int_0^\infty I(q) q^2 dq \quad (3)$$

The second moment, written in the form of Guinier relation, allows us to estimate the average size of scattering nonuniformities

$$I(q) = I_0 \exp(-q^2 R_g^2/3) \quad (4)$$

Here R_g is particle radius characterizing its shape and size. For a spherical particle with radius R_0 , $R_g^2 = \frac{3}{5} R_0^2$.

Analyzing the measured intensity in the coordinates $\ln(I)$, q^2 and using equation (4), we determined the average size of the formed carbon particles from the slope of the plot.

The SR beam intensity existing at the VEPP-3 storage turns out to be insufficient for the use of monochromatic spectrum in SAXS measurements because the intensity of scattered radiation is several orders of magnitude lower than that of the transmitted radiation, and because there is very small exposure (1 ns). In this connection, we used the SR beam with the initial polychromatic spectrum; its intensity was 2–3 orders of magnitude higher than in the case of monochromatic spectrum, and the wavelength varies from 0.15 to 0.04 nm (energy: from 6 to 30 keV).

To evaluate the signal recorded by the DIMEX detector, we carried out model experiments for the intensity of SAXS on spherical particles with the diameters of 2, 4, 10 and 20 nm situated in the THT charge 20 mm in diameter. Calculation was performed taking into account the spectrum of VEPP-3 (energy of electrons $E = 2$ GeV, wiggler with the induction of 2T) and the spectral sensitivity of DIMEX detector (5). The angular dependencies of SAXS for the particles with different diameters are shown in Figure 2. The angle is expressed in the channels of the detector (1 channel is equal to 0.1 mrad). One can see in

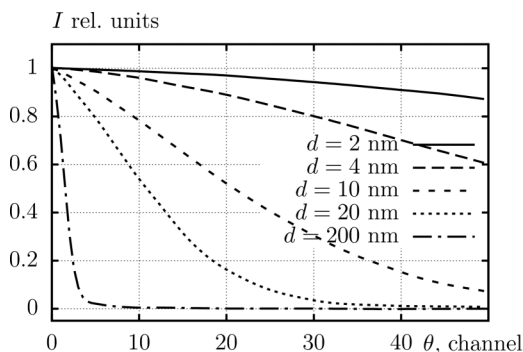


Figure 2. Dependence of SAXS signal on the diameter of scattering particles placed into the matrix composed of TNT.

this plot that the diameter of particles within the range from 2 to 100 nm can be determined from the slope of SAXS curves.

Setting and results of experiments

For dynamic experiments with SAXS registration, we used the measurement circuit described in (6) and shown in Figure 3. From the SR beam, with the help of the lower (K_1) and upper (K_2) knives (Kratki collimator), a band 0.4–1 mm high and 3–14 mm wide was formed on the central part of the charge. Before the detector, the direct flow was cut off by one or more lower knives (K_3). The deviated SAXS beams were recorded with the gas fast-response detector DIMEX (5).

The distance between the knives (K_1) and (K_2) was ~ 200 mm, the distance between knife K_2 and the explosive charge was ~ 700 mm, between the charge and the knife K_3 ~ 640 mm, between knife K_3 and detector ~ 260 mm. The angle range of SAXS measurements was $\sim 4 \cdot 10^{-4} - 10^{-2}$ rad. Such measurement range allows one to record SAXS from the particles having the size $\sim 2 - 70$ nm.

During one SR flare, the detector records all the channels (takes one frame) fixing the distribution of SAXS *versus* angle. Because the detonation front moves along axis Z at a constant speed, after the SR pulse period $T = 0.5 \mu\text{s}$ the detector records another

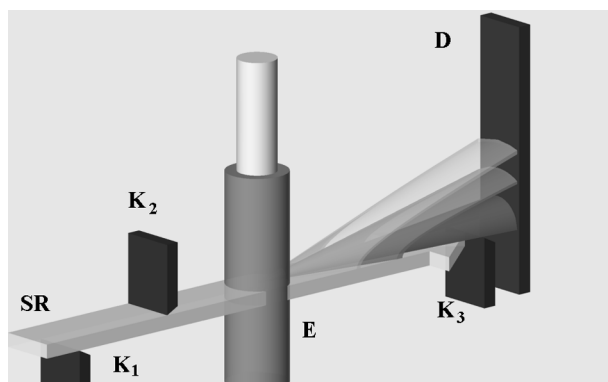


Figure 3. Scheme of the arrangement of experiments on the determination of SAXS dynamics in the detonation wave.

distribution of SAXS (one more frame), thus forming the sequence of SAXS signal distributions. In fact, this is the X-ray diffraction movie with the time shift of $0.5 \mu\text{s}$ and the duration of each frame 1ns .

We studied pressed charges based on TATB, the mixture of TNT50%+RDX50%, BTF 20mm in diameter and 30mm long. Ignition was performed with plasticized charge based on PETN.

Typical plots of the dynamics of SAXS signal summed over the whole angle range are shown in Figure 4a. The observed intense and long-lasting increase of the signal is determined both by the appearance of the scattering carbon phase and by the contrast increasing during the separation of detonation products.

Using the spatial distribution of density, determined in other experiments, one can normalize the obtained signal for the changing contrast (Figure 4b). Thus obtained signal is approximately proportional to the dynamics of the fraction of finally condensed carbon.

On the basis of these refined data, it is possible to estimate the time of carbon condensation: $2\mu\text{s}$.

The angular distributions of SAXS obtained in experiments (Figure 5) allow us to determine the dynamics of the average particle size using equation (4) (Figure 6).

The signal is minimal at the moment of detonation of the front passage; then a noticeable growth is observed. A substantial increase in the amplitude of SAXS signals is connected with the separation of detonation products and an increase in contrast. The change of the angular slope of the curve means the growth of scattering particles. Substantial "noise" at the curves is connected with a small amount of recorded photons (10–30 X-ray photons get into the detector channel).

It follows from these plots that the characteristic time of particle growth is about $2 \mu\text{s}$ for all the studied types of explosives. This is in agreement with the data on the time of growth of the total amount of the condensed phase.

Average particle size behind the detonation front depends on the type of explosives. For example, for TATB charges, nanoparticles with the size of $d \sim 2\text{nm}$ are detected at the detonation front; for the mixture TNT50%+RDX50%, $d \sim 5\text{nm}$; and for BTF, $d \sim 60\text{nm}$.

Conclusion

In detonation processes during condensation, carbon forms particles with different shapes and nonuniform phase composition. Complete deciphering of the structure of condensed phase is a complicated experimental and theoretical problem. The use of SAXS allows us to determine the dynamics of a number of average characteristics of the condensed phase.

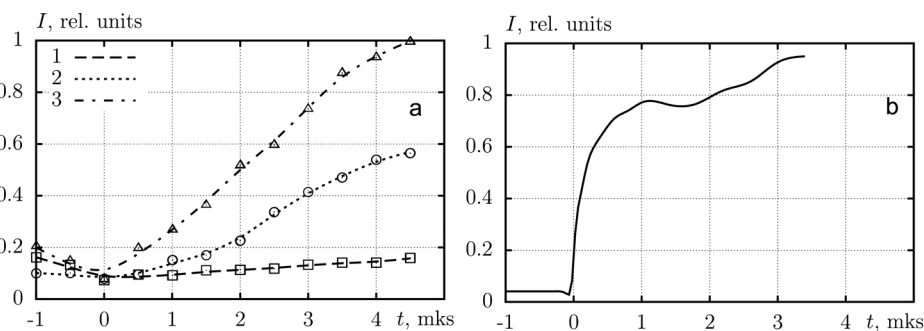


Figure 4. (a) Dependence of the SAXS signal summed over the whole angle range on time. (b) Dependence of the SAXS signal summed over the whole angle range divided by the contrast factor.

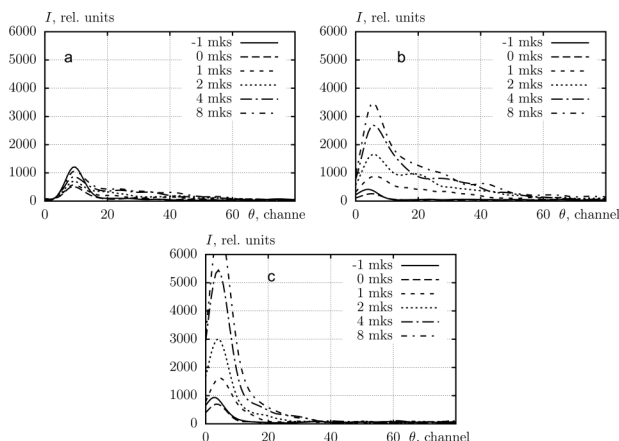


Figure 5. Dependence of the angular distribution of SAXS in different time moments during the detonation of the charges of different explosives: (a) based on triaminotrinitrobenzene (TATB), (b) composed of the mixture TNT50%+RDX50%, (c) benzotrifuroksane (BTF). Angle is plotted as the numbers of detector channels (1 channel = 0.1 mrad). The zero moment of time corresponds to the detonation front passage.

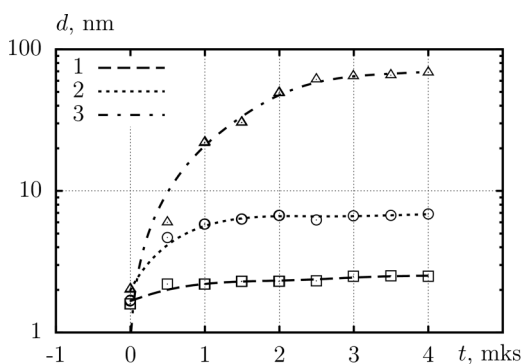


Figure 6. Dependence of nanoparticle sizes on time for the detonation of the charges of different explosives: 1 – BTF, 2 – composed of the mixture TNT50%+RDX50%, 3 – TATB.

On the basis of the integral intensity of SAXS, taking into account the changing contrast of the medium, we estimate the time of the formation of the total fraction of condensed carbon, without distinguishing shapes and sizes of the formed particles. For charges based on TATB with the diameter of 20 mm, it is approximately 2 μ s.

The dynamics of the average particle size is determined on the basis of the angular distribution of SAXS for the charges of different explosives: those based on TATB, composed of the mixture TNT50%+RDX50%, BTF.

Both methods give the upper estimation of the time of carbon condensation to be 2 μ s.

References

1. Viccelli, J.A. and Ree, F.H. (2000) Carbon particle phase transformation kinetics in detonation waves. *J. Appl. Phys.*, 88(2): 683–690.

2. Grebenkin, K.F., Taranik, M.V., and Zherebtsov, A.L. (2007) Slow energy release in detonation products of HMX-based explosives: Computer modeling and experimental effects. *Zababakhin Scientific Talks, Intern. Conf.* (Snezhinsk, Russia): 76.
3. Titov, V.M., Tolochko, B.P., Ten, K.A., Lukyanchikov, L.A., and Prueel, E.R. (2007) Where and when are nanodiamonds formed under explosion? *Diam. Relat. Mater.*, 16(12): 2009–2013.
4. Feigin, L.A. and Svergun, D.I. (1987) *Structure Analysis by Small-Angle X-Ray and Neutron Scattering*, Plenum Press: New York.
5. Aulchenko, V.M., Evdokov, O.V., Shekhtman, L.I., Ten, K.A., Tolochko, B.P., Zhogin, I.L., and Zhulanov, V.V. (2009) Current status and further improvements of the detector for imaging of explosions. *Nucl. Instrum. Meth. A*, 603(1–2): 73–75.
6. Ten, K.A., Aulchenko, V.M., Lukyanchikov, L.A., Prueel, E.R., Shekhtman, L.I., Tolochko, B.P., Zhogin, I.L., and Zhulanov, V.V. (2009) Application of introduced nano-diamonds for the study of carbon condensation during detonation of condensed explosives. *Nucl. Instrum. Meth. A*, 603(1–2): 102–104.